Planet. Space Sci., Vol. 24, pp. 589 to 604. Pergamon Press, 1976. Printed in Northern Ireland

ABSORPTION AND PHOTODISSOCIATION IN THE SCHUMANN–RUNGE BANDS OF MOLECULAR OXYGEN IN THE TERRESTRIAL ATMOSPHERE

G. KOCKARTS

Institut d'Aéronomie Spatiale de Belgique, 3 avenue Circulaire, B-1180 Bruxelles, Belgium

(*Received* 22 *December* 1975)

Abstract—The penetration in the terrestrial atmosphere of solar radiation corresponding to the spectral range of the Schumann–Runge bands of molecular oxygen is analyzed between 1750 and 2050 Å. The variation of the absorption cross section with temperature is taken into account and it is shown that average O_2 absorption cross sections cannot lead to correct photodissociation coefficients. Reduction factors are defined in order to simplify the computation of the molecular oxygen photodissociation and to permit a simple determination of the photodissociation coefficients of any minor constituent with smoothly varying absorption cross section. Examples are given for O_2, H_2O, CO_2, N_2O, HNO_3 and H_2O_2. Numerical approximations are developed for three types of spectral subdivisions: Schumann–Runge band intervals, 500 cm^{-1} and 10 Å intervals. The approximations are valid from the lower thermosphere down to the stratosphere and they can be applied for a wide range of atmospheric models and solar zenith distances.

INTRODUCTION

In the wavelength region between 1750 and 2050 Å, the major atmospheric absorption of solar radiation results from the numerous lines of the Schumann–Runge band system ($B^3\Sigma_u^- \leftarrow X^3\Sigma_g^-$) of molecular oxygen. Detailed computations of the penetration of solar radiation through the Schumann–Runge bands (Kockarts, 1971) require the knowledge of high resolution absorption cross sections (Ackerman *et al.*, 1970). This implies that a large amount of cross sections have to be stored in some way, especially since the absorption cross section is temperature dependent. Kockarts (1971) computed the absorption cross section at every 0.5 cm^{-1} in the Schumann–Runge bands and used 17 sets of 16,000 absorptions cross sections corresponding to temperatures which range from 160 to 320 K with 10 K interval.

Several attempts have been made to reduce the computer time and cost implied by such a procedure (Brinkmann, 1969; 1971; Anderson, 1971; Hudson and Mahle, 1972; Whitten and Turco, 1974; Fang *et al.*, 1974; Park, 1974). Any approximation should, however, be designed for a specific purpose. Two major problems are actually of practical significance: the photodissociation of O_2 itself and the absorption by O_2 which influences the photodissociation of several minor atmospheric constituents. These two question are discussed in this paper and approximate expressions are given to compute the solar penetration in the mesosphere and stratosphere, the photodissociation coefficients of O_2 and of the minor constituents which can be dissociated within the spectral range of the Schumann–Runge bands.

2. ABSORPTION CROSS SECTIONS AND SOLAR FLUXES

The major difficulty for using the absorption cross sections of molecular oxygen in the Schumann–Runge bands results from their large variation with wavelength and with temperature. The absorption cross sections discussed by Ackerman *et al.* (1970) change from 10^{-18} cm^2 at roughly 1750 Å to 10^{-23} cm^2 at 2050 Å. Within a specific band, variations of 3 order of magnitude are very common. As a consequence the optical depth is characterized by large variations over rather narrow wavelength intervals (Kockarts, 1971).

The molecular oxygen absorption cross sections in the Schumann–Runge bands essentially depend on various molecular parameters and on one atmospheric parameter, namely the temperature.

The molecular parameters are the line positions, the line widths and the band integrated absorption coefficients which are related to the band oscillator strengths. In the present paper, the molecular parameters are identical to the values used previously (Ackerman *et al.*, 1970; Biaumé, 1972a, b; Kockarts, 1972). The band oscillator strengths adopted by Biaumé (1972b) are in very good agreement with the values computed by Allison *et al.* (1971) and they also agree closely with the electron impact values obtained by Huebner *et al.* (1975)

between the vibrational levels $v' = 4$ and $v' = 11$. In their computation of the O_2 photodissociation coefficient, Hudson and Mahle (1972) adopted similar oscillator strengths except for $v' = 13$, 14 and 17–19. It should be noted that for $v' = 13$ and 14 there is also a very large discrepancy between the line widths of Hudson and Mahle (1972) and the values used by Ackerman *et al.* (1970). The important problem of line width determination has been analyzed theoretically by Julienne and Krauss (1975). They showed that a rather large discrepancy exists between theoretical and experimental line widths for $v' = 5$–11 and they suggest that the difference could be due to line blending. Apparently, more experimental and theoretical work is needed before this question can be solved. The agreement between the O_2 photodissociation coefficient (Kockarts, 1971) computed with the line widths of Ackerman *et al.* (1970) and the values obtained by Hudson and Mahle (1972) with their line widths is, however, satisfactory. Furthermore, the water vapor photodissociation coefficient obtained by Fang *et al.* (1974) with the line widths of Hudson and Mahle (1972) agrees also with the values computed by Kockarts (1971). It seems, therefore, that the line width problem is not so crucial when photodissociation coefficients of O_2 and other minor constituents are computed over the whole Schumann–Runge bands. This is, however, not correct for a computation at a specific wavelength. Finally, it is worthwhile to mention that more precise molecular constants for the Schumann–Runge system have been obtained by Creek and Nicholls (1975). These constants can be used to compute line positions. Ackerman *et al.* (1970), however, used experimental line positions for the $v'' = 0$ progression and molecular constants were only used to compute the line positions for the $v'' = 1$ bands. A calculation made with the new values of Creek and Nicholls (1975) indicates that up to the lines 13 R and 13 P of the $v'' = 1$ bands the agreement is very good, of the order of $0.1\ \text{cm}^{-1}$. For higher quantum numbers in the R and P branches, larger differences occur. This implies again that with these new molecular constants, changes can occur at specific wavelengths within a band. Since the purpose of the present paper is to provide *average* photodissociation coefficients, the previous molecular parameters given by Ackerman *et al.* (1970) are not modified in the following computations. When all the molecular parameters discussed previously are known with better accuracy, it will be necessary to recompute the detailed absorption cross sections. This is particularly true for the analysis of future *in situ* observations made with a resolution better than $0.5\ \text{cm}^{-1}$, i.e. approx. 0.02 Å in the wavelength range of the Schumann–Runge bands system.

Since the temperature in the homosphere can vary between 160 and 300 K at different levels, the influence on the O_2 absorption cross section will be discussed in this temperature range. With the expressions used by Ackerman *et al.* (1970) and by Kockarts (1972), it can be shown that the ratio $\sigma(T_1)/\sigma(T_2)$ of the absorption cross for the temperatures T_1 and T_2 is given by:

$$\sigma(T_1)/\sigma(T_2) = \frac{T_2 F(T_1, v'')}{T_1 F(T_2, v'')} \exp\left[-\alpha\left(\frac{1}{T_1} - \frac{1}{T_2}\right)\right] \quad (1)$$

where $F(T_1, v'')$ and $F(T_2, v'')$ are respectively the relative numbers of molecules in the vibrational level v'' for T_1 and T_2 (Herzberg, 1950). The quantity α is given by:

$$\alpha = (hc/k) B_{v''} N''(N'' + 1), \quad (2)$$

where h is Planck's constant, c is the speed of light, k is Boltzmann's constant, $B_{v''}$ is the rotational constant of the vibrational level v'' and N'' is the rotational quantum number of the v'' levels which takes the values 1, 3, 5, 7 .... Expression (1) is only rigorously valid for the absorption cross section resulting from a single line and it reflects the variation of the relative intensity of the various lines in a specific band. For the lowest vibrational level $v'' = 0$, $F(T_1, 0) = F(T_2, 0) = 1$. Taking $B_0 = 1.43771\ \text{cm}^{-1}$ (Creek and Nicholls, 1975) and introducing the other numerical constants in (2), expression (1) leads to the ratio

$$\sigma(T_1)/\sigma(T_2) = (T_2/T_1) \exp\left[-1.955\ N''(N'' + 1)\right] \quad (3)$$

for the cross sections in a P or R branch of the $v'' = 0$ bands. With $T_1 = 150$ K and $T_2 = 300$ K, expression (3) shows that $\sigma(150)$ is greater than $\sigma(300)$ for $N'' < 11$ and that the inverse relation occurs for $N'' > 11$. Therefore, the absorption cross section is a decreasing function of the temperature near the band heads and an increasing function of the temperature from a certain value of N'' which depends on the temperature. The real behavior of the cross section is a little more complicated since at a specific wavelength the cross section results from the overlapping of several lines. Furthermore the $v'' = 1$ progression cannot be neglected for temperatures above 200 K. Figure 1 shows variations of the absorption cross section as a function of temperature at various wavelengths in the P branch of the 4–0 band. The characteristics deduced from

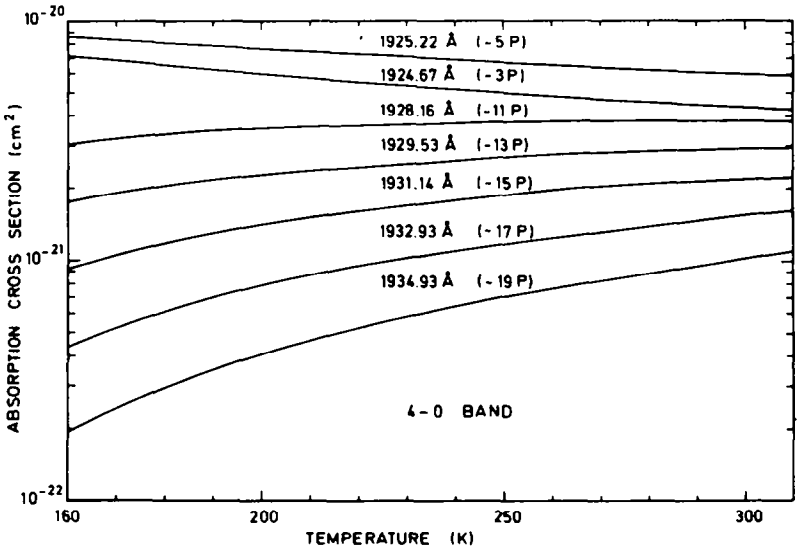

FIG. 1. ABSORPTION CROSS SECTIONS AT SPECIFIC WAVELENGTHS IN THE 4–0 BAND OF THE O_2 SCHUMANN-RUNGE SYSTEM AS A FUNCTION OF TEMPERATURE.
The wavelengths correspond to various lines in the P branch.

expression (3) are found in Fig. 1; e.g. the cross section becomes an increasing function of temperature at the 11 P line and the cross section increases by a factor of 5 between 160 and 300 K for the 19 P line. Since there is a reversal in the temperature dependence within each band, it is instructive to examine the behavior of the mean absorption cross section computed for each band. These mean absorption cross sections for two extreme temperatures, namely 160 and 300 K are given in Fig. 2 which shows that there is no strong temperature dependence. The first impression is, therefore, that such values are appropriate for the computation of solar radiation absorption and of photodissociation coefficients. However, it will be shown in the next section which type of error is introduced when such mean absorption cross sections are used. The errors which arise from the use of mean absorption cross sections are actually a consequence of very large standard deviations which characterize such mean absorption cross sections. As an example, the mean absorption cross section for 250 K in the 9–0 band is 2.0×10^{-20} cm^2 with a S.D. of 5.4×10^{-20} cm^2. It appears, therefore, that the temperature dependence of the absorption cross section should be included in any detailed computations, although Park (1974) used only absorption cross sections at 250 K for computing O_2 and H_2O photodissociation coefficients and neglected the $v''=1$ progression.

High resolutions solar spectra are now becoming available in the Schumann–Runge spectral region. Recently, Samain and Simon (1976) used a solar spectrum obtained by Samain *et al.* (1975) at the center of the solar disk, with a resolution of 0.4 Å, to determine the whole solar disk flux between 1500 and 2100 Å using center to limb darkening curves. The spectral region of the Schumann–Runge bands is illustrated by Fig. 3. Even if the structure is rather well known, errors in the absolute calibration of the measured solar fluxes are, however, not excluded. The average error is estimated to be less than ±25% (Samain *et al.*, 1975). The spectrum of Fig. 3 has been interpolated every 0.5 cm^{-1} when detailed computations are required. The origins of the bands in the Schumann–Runge system are also indicated on Fig. 3 by the upper vibrational level v' in order to show where the fine structure of the solar spectrum could play a role.

For the calculation of photodissociation coefficients of minor constituents with smoothly varying cross sections, we can use, however, the band average fluxes as given in Table 1 without making an important error. The solar fluxes quoted in Table 1 are given as an example which should allow future comparisons with other values. It is, however, important to note that the approximations developed in the present paper are independent of the exact values of the solar fluxes.

The wavenumbers of the band origins, rounded

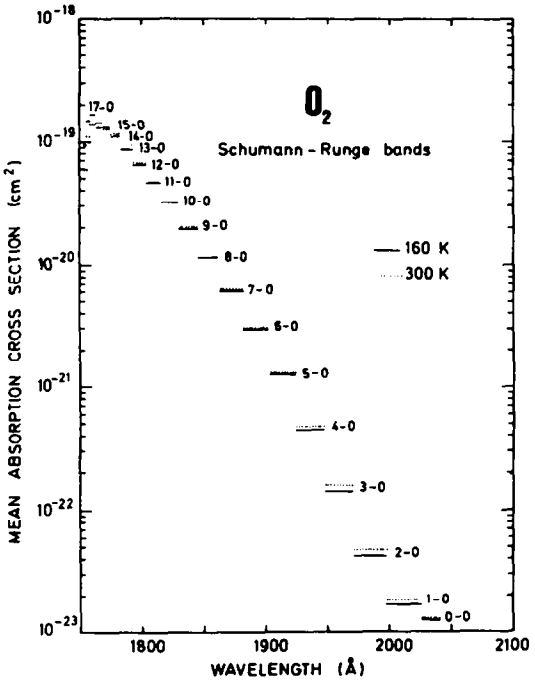

FIG. 2. MEAN ABSORPTION CROSS SECTIONS IN THE VARIOUS BANDS OF THE O_2 SCHUMANN-RUNGE SYSTEM FOR TWO EXTREME STRATOSPHERIC AND MESOSPHERIC TEMPERATURES, NAMELY 160 AND 300 K.

off to half a wavenumber, are also given in Table 1, as well as the average absorption cross sections for the minor constituents which will be considered in the next section. The H_2O and H_2O_2 absorption cross sections are obtained by interpolation from the values used by Nicolet (1971). The carbon dioxide absorption cross sections are from Shemansky (1972). The N_2O values result from interpolation in the values adopted by Nicolet and Peetermans (1972) whereas the nitric acid data are taken from Biaumé (1973).

3. REDUCTION FACTORS AND PHOTODISSOCIATION COEFFICIENTS

In the lower thermosphere and mesosphere, molecular oxygen is certainly the principal atmospheric constituent absorbing the solar radiation in the Schumann–Runge spectral region. In the stratosphere, however, the absorption by ozone cannot be neglected. The expressions presented in this section consider only the absorption by molecular oxygen and it will be indicated how the ozone effect can be taken into account. Such a procedure is adopted to simplify the discussion pertinent to the molecular oxygen absorption.

The Schumann–Runge system is first divided in 20 wavelengths intervals, from (19–0) to (0–0),

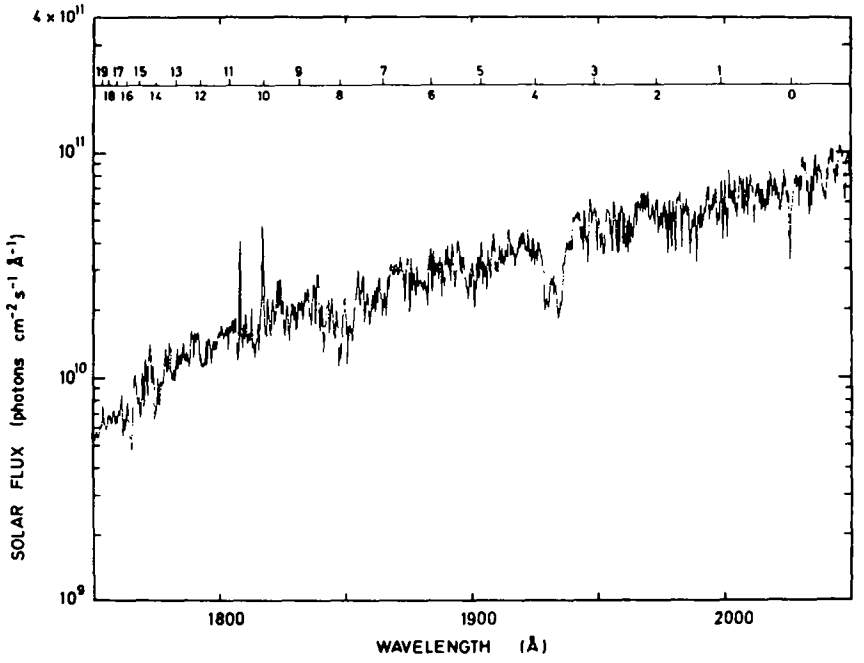

FIG. 3. SOLAR FLUX IN THE O_2 SCHUMANN-RUNGE SPECTRAL REGION AS DETERMINED BY SAMAIN AND SIMON (1976).
Band origins are indicated by the upper vibrational quantum number.

TABLE 1. AVERAGE SOLAR FLUXES AND AVERAGE ABSORPTION CROSS SECTIONS OF MINOR CONSTITUENTS IN THE SPECTRAL RANGE OF THE SCHUMANN–RUNGE BANDS OF O_2

Bands (v'-v'')	Wavenumbers (cm^{-1})	Wavelengths (Å)	Photons ($cm^{-2}s^{-1}\Delta\lambda^{-1}$)	Absorption cross sections (cm^2) H_2O	CO_2	N_2O	H_2O_2	HNO_3
19-0	57030.5	1753.45	1.50×10^{10}	2.40×10^{-18}	5.18×10^{-21}	1.18×10^{-19}	–	–
18-0	56954.5	1755.79	2.10	2.35	4.52	1.19	–	–
17-0	56852.5	1758.94	2.81	2.25	4.51	1.20	–	–
16-0	56719.5	1763.06	3.84	2.20	3.81	1.21	–	–
15-0	56550.5	1768.33	6.40	1.95	3.33	1.23	–	–
14-0	56340.5	1774.92	8.38	1.70	2.74	1.30	–	–
13-0	56085.5	1782.99	1.26×10^{11}	1.45	1.78	1.32	–	–
12-0	55784.5	1792.61	1.56	8.10×10^{-19}	1.48	1.37	–	–
11-0	55439.0	1803.78	2.08	4.20	1.10	1.40	1.60×10^{-18}	–
10-0	55051.0	1816.50	2.91	1.90	7.91×10^{-22}	1.40	1.45	–
9-0	54622.0	1830.76	3.13	7.40×10^{-20}	5.19	1.35	1.38	–
8-0	54136.5	1846.50	3.42	3.80	3.00	1.30	1.02	–
7-0	53656.5	1863.71	4.98	1.80	1.59	1.22	8.80×10^{-19}	1.60×10^{-17}
6-0	53123.0	1882.42	6.02	7.20×10^{-21}	8.41×10^{-23}	1.12	8.00	1.50
5-0	52561.5	1902.53	7.58	2.90	4.76	1.05	7.00	1.47
4-0	51970.0	1924.19	8.15	9.80×10^{-22}	2.45	8.80×10^{-20}	6.20	1.25
3-0	51352.5	1947.32	1.22×10^{12}	3.70	1.32	7.00	5.80	9.20×10^{-18}
2-0	50711.0	1971.96	1.38	1.25	3.97×10^{-24}	4.80	5.30	6.70
1-0	50046.0	1998.16	1.79	3.70×10^{-23}	1.44	3.40	4.95	4.65
0-0	49356.0	2026.01	1.09	–	8.62×10^{-25}	2.45	4.70	3.20

each one commencing at a band origin and the last one ending at 49000 cm^{-1}, i.e. 2040.8 Å. Furthermore, each of the 20 band intervals b is divided in a certain number n_b of subintervals where the O_2 absorption cross section σ_{ib} is computed every 0.5 cm^{-1}. If $\phi_{ib}(\infty)$ represents the solar flux available at the top of the atmosphere in a subinterval, the solar flux $\phi_b(z)$ reaching the height z in a band b is given by

$$\phi_b(z) = \sum_{i=1}^{n_b} \phi_{ib}(\infty) \exp(-\tau_{ib}). \tag{4}$$

The optical depth τ_{ib} is given by:

$$\tau_{ib} = \int_z^\infty \sigma_{ib} n(O_2)\, ds, \tag{5}$$

where $n(O_2)$ is the molecular oxygen concentration and the element ds is taken along the path of the radiation. Since the absorption cross section is temperature dependent, σ_{ib} must be kept under the integral sign, contrary to the formulation of Park (1974). The photodissociation coefficient of a minor constituent M for which the photodissociation cross section $\sigma_b(M)$ can be considered as constant over a band interval is then simply

$$J_b(M) = \sigma_b(M)\phi_b(z), \tag{6}$$

where $\phi_b(z)$ is given by equation (4).

The photodissociation coefficient of molecular oxygen $J_b(O_2)$ in one band b of the Schumann–Runge system can be written

$$J_b(O_2) = \sum_{i=1}^{n_b} \varepsilon_b \sigma_{ib} \phi_{ib}(\infty) e^{-\tau_{ib}}. \tag{7}$$

In expression (7), ε_b represents the predissociation probability in a band b. This probability is not yet known and it will be assumed here that ε_b is equal to unity. The difference of a predissociation effect starting at $v' = 0$ or at $v' > 3$ has been considered by Kockarts (1971).

From expressions (4), (6) and (7), it appears that no further significant algebraic manipulations can be made, if the fine structure of the solar spectrum is to be taken into account. In order to show the relative importance of the various bands as a function of height, Fig. 4 gives different fractions of the O_2 Schumann–Runge photodissociation coefficient computed with the solar fluxes corresponding to the detailed solar spectrum of Samain and Simon (1976). The absorption and photodissociation in the O_2 Herzberg continuum for $\lambda < 2424$ Å can lead to a significant contribution mainly for wavelengths above 1900 Å. Therefore, the absorption cross sections deduced by Jarmain and Nicholls (1967) for the Herzberg continuum are added to the Schumann–Runge bands absorption cross sections over the whole spectral range. Constant values are adopted for spectral intervals of 200 cm^{-1} (Kockarts, 1972). The four curves correspond respectively to the following spectral intervals: 1753.46–1774.92 Å for bands 19–0 to 15–0, 1774.92–1830.76 Å for bands 14–0 to 10–0, 1830.76–1924.19 Å for bands 9–0 to 5–0, and 1924.19–2040.82 Å for bands 4–0 to 0–0. The computation is made for an overhead Sun with the temperature profile and the molecular oxygen concentration from the U.S. Standard Atmosphere 1962 (COESA, 1962). It can be seen that the effect of the short wavelength spectral range is almost

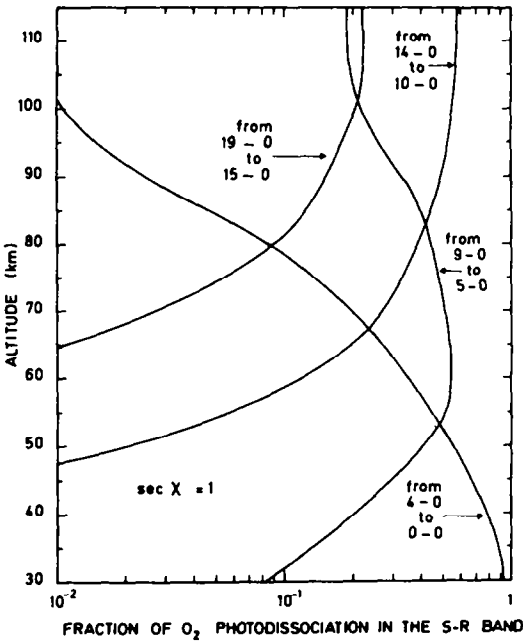

FIG. 4. VERTICAL DISTRIBUTION OF VARIOUS FRACTIONS OF O_2 PHOTODISSOCIATION FOR 4 GROUPS OF BANDS OF THE SCHUMANN-RUNGE SYSTEM: 19–0 TO 15–0, 14–0 TO 10–0, 9–0 TO 5–0 AND 4-0 TO 0–0.
Overhead Sun conditions.

entirely negligible below the mesopause. In the lower thermosphere the bands 14–0 to 10–0 give the major contribution to the dissociation of the Schumann–Runge band system. The bands 9–0 to 5–0 have their dominant effect in the mesosphere, whereas the bands 4–0 to 0–0 play the major role in the stratosphere. The $v''=1$ progression is included in the results shown in Fig. 4.

A major simplification is possible in expressions (4) and (7) when use is made of a band average solar flux $\phi_b(\infty)$ such that

$$\phi_b(\infty)=\sum_{i=1}^{n_b}\phi_{ib}(\infty)=n_b\phi_{ib}'(\infty). \tag{8}$$

When the flux $\phi_{ib}'(\infty)$ defined by (8), is used in Equations (4) and (7) instead of $\phi_{ib}(\infty)$ one obtains

$$\phi_b(z)=\phi_b(\infty)\frac{1}{n_b}\sum_{i=1}^{n_b}\exp(-\tau_{ib}) \tag{9}$$

and

$$J_b(O_2)=\phi_b(\infty)\frac{1}{n_b}\sum_{i=1}^{n_b}\varepsilon_b\sigma_{ib}\exp(-\tau_{ib}). \tag{10}$$

Total photodissociation coefficients computed with Equation (10) differ by less than 1% from those obtained with Equation (7). Inspection of the solar spectrum (Fig. 3) shows, however, that in the 11–0 and 10–0 bands where the two SiII emission lines are observed and in the 4–0 band where the AlI absorption occurs, a detailed computation is preferable when one looks only for specific effects in these spectral intervals.

The reduction factors $R_b(M)$ and $R_b(O_2)$ introduced by Kockarts (1971) are now defined for each band b as

$$R_b(M)=\frac{1}{n_b}\sum_{i=1}^{n_b}\exp(-\tau_{ib}) \tag{11}$$

and

$$R_b(O_2)=\frac{1}{n_b}\sum_{i=1}^{n_b}\varepsilon_b\sigma_{ib}\exp(-\tau_{ib}). \tag{12}$$

The dimensionless reduction factor $R_b(M)$ is the equivalent of the transmission function used by Fang *et al.* (1974) and $R_b(O_2)$ in cm^2 is equivalent to the expression used by Fang *et al.* (1974) for the computation of the O_2 photodissociation. Similar expressions have also been by adopted by Park (1974) without taking into account the temperature dependence of the absorption cross section. Figures 5 and 6 give examples of the reduction factors $R_b(O_2)$ and $R_b(M)$ as a function of the O_2 total content. The computation is made with the parameters of the U.S. Standard Atmosphere 1962 (COESA, 1962). The altitude scale corresponds to overhead Sun conditions. The dashed curves give the results when the temperature is arbitrarily assumed constant for a range of O_2 total content between 10^{17} and $10^{23}\,cm^{-2}$. Although the differences between the constant temperature curves and the exact computation is not very large in the case of $R_b(O_2)$ (see Fig. 5), it is clear from Fig. 6 that a constant temperature is an unrealistic assumption in the case of $R_b(M)$. Similar results are obtained for the other bands of the Schumann–Runge system.

When the reduction factors are known, the computation of the solar flux $\phi_b(z)$ reaching the height z, of the O_2 photodissociation coefficient $J_b(O_2)$ and of the photodissociation coefficient $J_b(M)$ for a minor constituent M is straightforward with the following expressions

$$\phi_b(z)=\phi_b(\infty)R_b(M)\exp[-\tau_b(O_3)] \tag{13}$$

$$J_b(O_2)=\phi_b(\infty)R_b(O_2)\exp[-\tau_b(O_3)] \tag{14}$$

$$J_b(M)=\phi_b(\infty)\sigma_b(M)R_b(M)\exp[-\tau_b(O_3)]. \tag{15}$$

The effect resulting from the ozone absorption is taken into account by the factor $\exp[-\tau_b(O_3)]$ where $\tau_b(O_3)$ is the ozone optical depth at height z. The ozone absorption cross sections are taken from Ackerman (1971).

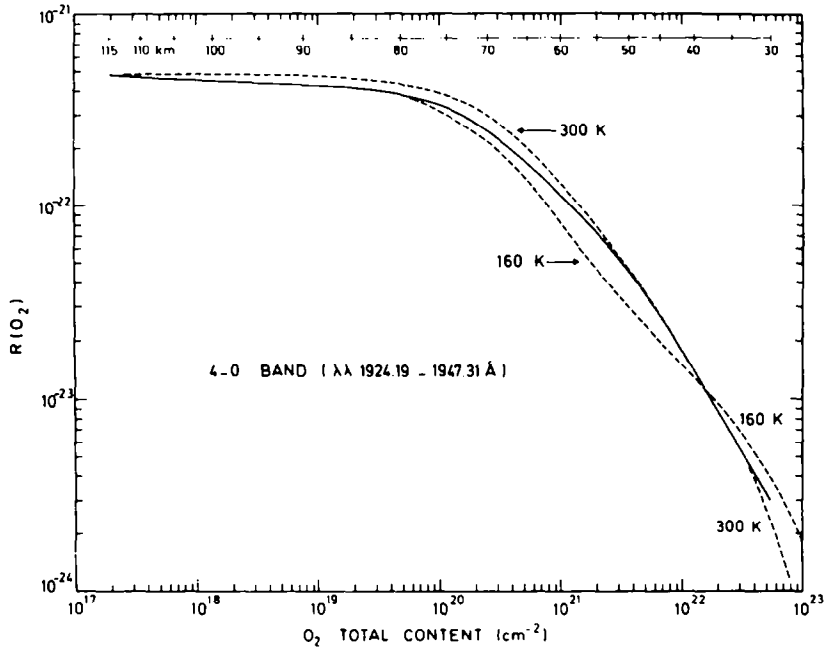

FIG. 5. COMPARISON OF THE REDUCTION FACTOR $R_b(O_2)$ IN THE 4–0 BAND COMPUTED WITH TEMPERATURE DEPENDENT CROSS SECTIONS (FULL CURVE) AND WITH CONSTANT TEMPERATURE (160 AND 300 K) CROSS SECTIONS.

Overhead sun conditions.

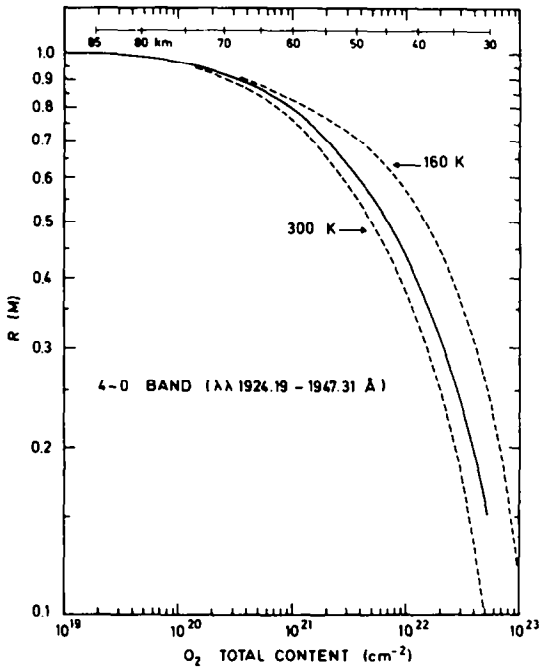

FIG. 6. COMPARISON OF THE REDUCTION FACTOR $R_b(M)$ IN THE 4–0 BAND COMPUTED WITH TEMPERATURE DEPENDENT CROSS SECTIONS (FULL CURVE) AND WITH CONSTANT TEMPERATURE (160 AND 300 K).

Overhead Sun conditions.

The addition of the 20 partial coefficients obtained from expression (14) leads to the O_2 photodissociation coefficient shown on Fig. 7. The dashed curve represents the result obtained with the mean absorption cross sections shown on Fig. 2. Errors larger than a factor of two appear over an extended range of the O_2 total content. In the upper stratosphere and lower mesosphere where the O_2 total content ranges from 10^{22} to 10^{21} cm^{-2}, there is an excellent agreement. The ozone distribution adopted in the computation of Fig. 7 is taken from Nicolet (1975) and it affects the results only below 40 km.

The photodissociation coefficients of several minor constituents, as shown in Fig. 8, are obtained when expression (15) is used for each band of the Schumann–Runge system and when solar fluxes and absorption cross sections given in Table 1 are adopted. As in Fig. 7, the dashed curves of Fig. 8 are also computed with the mean cross sections defined in the preceding section. It is clear that these mean cross sections cannot be used for any calculation of the photodissociation of minor constituents in the Schumann–Runge band spectral range. The use of mean cross sections always leads to a large underestimation of the photodissociation coefficients as has already been noticed by Fang *et*

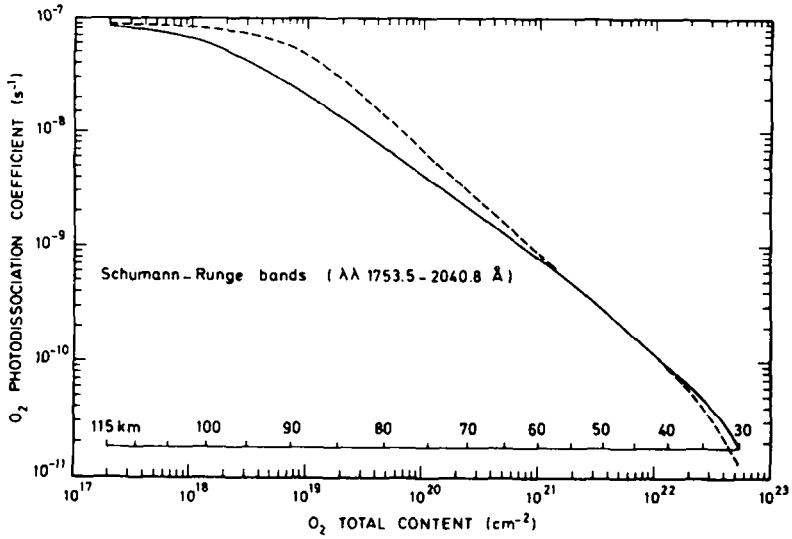

FIG. 7. O_2 PHOTODISSOCIATION COEFFICIENT IN THE SCHUMANN–RUNGE BANDS AS A FUNCTION OF THE O_2 TOTAL CONTENT (FULL CURVE).

The dashed curve is obtained with the mean absorption cross sections of Fig. 2. Overhead Sun conditions.

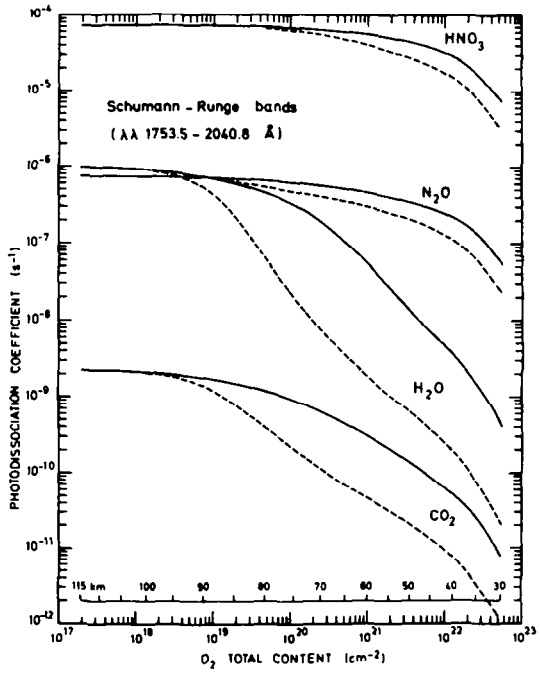

FIG. 8. PHOTODISSOCIATION COEFFICIENTS OF HNO_3, N_2O, H_2O AND CO_2 IN THE SCHUMANN-RUNGE SPECTRAL REGION AS A FUNCTION OF THE O_2 TOTAL CONTENT (FULL CURVES).

The dashed curves are obtained with the mean absorption cross sections of Fig. 2. Overhead Sun conditions.

al. (1974). The difference between the present values and those given by Kockarts (1971) for H_2O and by Banks and Kockarts (1973) for CO_2 is due essentially to the adoption of different values (Samain and Simon, 1976) for the solar fluxes.

In order to illustrate the role of the photodissociation in the spectral range of the Schumann–Runge bands, Fig. 9 shows the vertical distribution of the ratio of the photodissociation coefficient in the Schumann–Runge wavelength region (J_{S-R}) and the total photodissociation coefficient (J_{total}). The solar fluxes outside of the Schumann–Runge bands have been adopted from Simon (1976). Between approx. 65 and 95 km, the predissociation in the Schumann–Runge bands is the major dissociative process for O_2 for overhead Sun conditions. In the stratosphere above 30 km, the photodissociation in the Schumann–Runge wavelength region contributes roughly by 50% to the photodissociation of nitric acid and of nitrous oxide. Below 60 km the photodissociation of CO_2 and H_2O is entirely due to solar radiation which penetrates in the Schumann–Runge bands. For H_2O_2, the contribution from the Schumann–Runge wavelength region is practically negligible.

Before introducing numerical approximations, it is useful to compare the absorption in the Herzberg continuum which starts at 2424 Å with the absorption in the Schumann–Runge bands which begin at

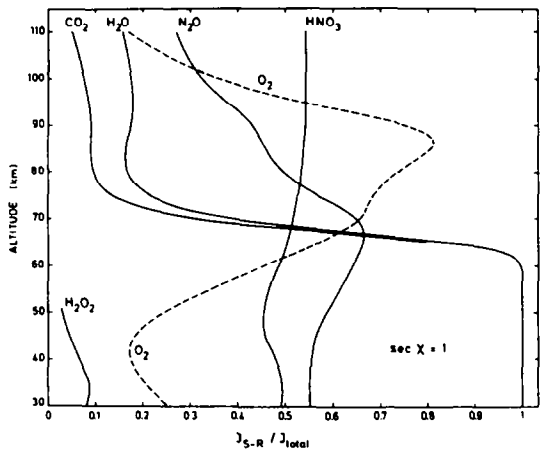

FIG. 9. RATIOS OF PHOTODISSOCIATION COEFFICIENTS IN THE SCHUMANN–RUNGE SPECTRAL RANGE (J_{S-R}) AND THE TOTAL PHOTODISSOCIATION COEFFICIENTS (J_{total}) VS HEIGHT FOR OVERHEAD SUN CONDITIONS.

2040 Å. From $\lambda \simeq 2040$ Å, corresponding to the 0–0 band of the Schumann–Runge system, the absorption cross section of the Herzberg continuum increases from 1.15×10^{-23} cm^2 to its maximum of 1.30×10^{-23} cm^2 (Jarmain and Nicholls, 1967) near $\lambda = 1950$ Å which corresponds to the Schumann–Runge band 3–0. Since it is not yet established whether or not predissociation occurs in this spectral region, the contribution of the spectral range λλ 1950–2040 Å to the O_2 photodissociation must be studied with and without the action of a predissociation process in the Schumann–Runge bands 0–0 to 3–0 in addition to the normal photodissociation in the Herzberg continuum. Figure 10 shows

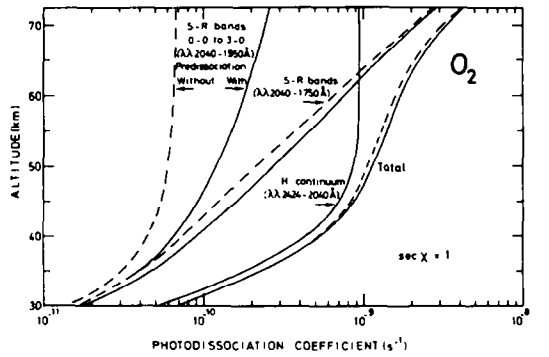

FIG. 10. VERTICAL DISTRIBUTION OF THE O_2 PHOTODISSOCIATION COEFFICIENT FOR OVERHEAD SUN CONDITIONS.
Contribution of the Herzberg continuum (H) from 2424 to 2040 Å and the Schumann–Runge bands (S–R) from 2040 to 1750 Å. The dashed curves correspond to the absence predissociation in the 0–0 to 3–0 bands (λλ 2040–1950 Å) of the Schumann–Runge system.

the relative importance of the photodissociation due to the Schumann–Runge bands and to the Herzberg continuum between the threshold at 2424 and about 2040 Å where the 0–0 band starts. Two cases have been considered for the contribution of the Schumann–Runge bands: the full curve corresponds to complete predissociation in the whole band system and the dashed curve ignores predissociation in the 0–0 to 3–0 bands, but it takes into account the photodissociation in the underlying Herzberg continuum. In both cases absorption of the Herzberg continuum is included in the optical depth. Although the absence of predissociation in the 0–0 to 3–0 bands can reduce the photodissociation coefficient in the Schumann–Runge bands by 25% at 45 km, the reduction of the total O_2 photodissociation coefficient is, however, less than 5% over the whole height range, as can be seen on Fig. 10.

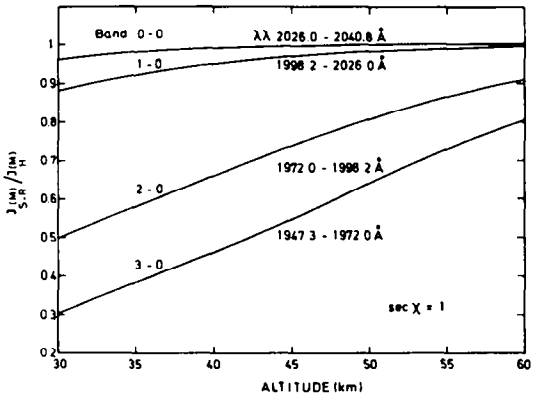

FIG. 11. RATIO OF THE CORRECT PHOTODISSOCIATION COEFFICIENT $J_{S-R}(M)$ AND THE COEFFICIENT $J_H(M)$ RESULTING FROM ABSORPTION BY THE HERZBERG CONTINUUM IN THE 0–0, 1–0, 2-0 AND 3–0 BANDS OF THE SCHUMANN–RUNGE SYSTEM.
The curves are valid for any minor constituent with constant absorption cross section over each band interval. Overhead Sun conditions.

As far as the minor constituents are concerned, the problem is different since it is only an absorption process which limits the penetration of solar radiation and affects in this way the value of the photodissociation coefficient. If the correct photodissociation coefficient of a minor constituent involving the total absorption in a certain band interval is designated by $J_{S-R}(M)$ and if $J_H(M)$ corresponds to the effect of the Herzberg continuum absorption in the same spectral range, the ratio $J_{S-R}(M)/J_H(M)$ does not depend on the absorption cross-section of the minor constituent. Such a ratio is given on Figure 11 as a function of height for the

0–0 to 3–0 bands. It appears that without the effect of the absorption by the lines of the Schumann–Runge bands 0–0 to 3–0, the photodissociation coefficient is always overestimated, i.e. $J_{S-R}(M)/J_H(M)<1$. Below 2000 Å, absorption by the lines of the Schumann–Runge bands must be taken into account. It is, therefore, clear that the absorption of the Schumann–Runge bands plays an important role not only in the mesosphere, but also in the stratosphere where several minor constituents are subject to photodissociation processes at wavelengths shorter than 2000 Å.

4. NUMERICAL APPROXIMATIONS FOR EACH BAND

It has been shown in the preceding section how the exact reduction factors can be applied to the Earth's atmosphere. Since $R_b(O_2)$ and $R_b(M)$ result from a detailed lengthy calculation, it is interesting to determine the approximation which can be valid for a large range of atmospheric conditions. A tabulation of the reduction factors as a function of height or O_2 total content is not very handy, since it requires important computer storage and subsequent interpolations. The temperature dependence of the transmittance of solar radiation and of the rate of dissociation is fitted by Hudson and Mahle (1972) through an empirical relation for which the numerical coefficients are given in tabular form as a function of the O_2 total content. Park (1974) gives a graphical representation of two sets of equivalent absorption cross sections as a function of the O_2 total content for one temperature. The technique adopted by Fang *et al.* (1974) is more practical but it requires, nevertheless, a numerical integration in order to obtain photodissociation coefficients as a function of the O_2 total content.

A good analytical approximation of the natural logarithm of the present reduction factors is given by:

$$\ln R_b^*(x) = -a \exp[c_1(x-x_0) + c_2(x-x_0)^2 + \ldots + c_6(x-x_0)^6], \quad (16)$$

where x is the natural logarithm of the total content of molecular oxygen. The numerical coefficients x_0, a, c_1 through c_6 are obtained through a least square fitting and are given in Tables 2 and 3 for the two reduction factors deduced for each band. These coefficients imply that the O_2 total content is expressed in molecules cm^{-2}. The coefficients $x_0 = \int_{z_0}^{\infty} n(O_2)\, ds$ have been chosen in a way such that the corresponding reduction factor is reduced by a factor of 1000. This implies that in each band, radiation is considered as completely absorbed when the average optical depth is greater than 6.9. For the bands $v'<4$, x_0 corresponds to the height of 30 km for an overhead Sun, since the computations have been stopped at that altitude. The highest altitude for which the present approximation is valid corresponds to an O_2 total content of 1.94×10^{17} cm^{-2}, i.e. an altitude of 115 km in the 45°N U.S. Standard Atmosphere for overhead Sun conditions.

For a given O_2 total content, the reduction factors $R_b^*(O_2)$ and $R_b^*(M)$ can be immediately computed from expression (16) and Tables 2 and 3. The error δ resulting from the use of expression (16) depends on the O_2 total content and has been

TABLE 2. COEFFICIENTS FOR THE REDUCTION FACTORS $R_b^*(M)$ IN FORMULA (16)

Band	x_o	a	c_1	c_2	c_3	c_4	c_5	c_6
19 - 0	48.5010	6.31710 (+0)*	6.08574 (-1)	2.97159 (-2)	5.09179 (-3)	–	–	–
18 - 0	47.8366	7.00050 (+0)	6.46284 (-1)	2.67214 (-2)	- 6.61165 (-3)	- 2.90019 (-3)	- 1.88591 (-4)	–
17 - 0	48.5010	6.89325 (+0)	5.76123 (-1)	6.46560 (-2)	1.20411 (-2)	4.25760 (-4)	–	–
16 - 0	48.3707	6.82169 (+0)	5.52366 (-1)	1.41801 (-2)	- 3.82459 (-3)	- 1.54704 (-3)	- 8.62462 (-5)	–
15 - 0	48.8862	6.84542 (+0)	7.04170 (-1)	7.90948 (-2)	4.21208 (-3)	- 1.05961 (-3)	- 7.41033 (-5)	–
14 - 0	49.1384	6.62131 (+0)	6.93027 (-1)	6.68624 (-2)	6.29880 (-3)	–	–	–
13 - 0	49.3872	6.74723 (+0)	6.28943 (-1)	- 2.45785 (-2)	- 2.08983 (-2)	- 3.09907 (-3)	- 1.24542 (-4)	–
12 - 0	49.5111	6.77155 (+0)	6.92233 (-1)	2.13024 (-2)	- 2.32312 (-3)	6.34869 (-4)	2.40848 (-4)	1.36871 (-5)
11 - 0	50.2588	6.74874 (+0)	5.26218 (-1)	- 2.16025 (-2)	- 8.38765 (-3)	- 1.20850 (-4)	1.50742 (-4)	9.13218 (-6)
10 - 0	50.9126	7.13157 (+0)	5.88084 (-1)	9.18305 (-3)	- 9.82008 (-4)	6.14794 (-4)	1.55366 (-4)	7.40423 (-6)
9 - 0	52.3372	6.38994 (+0)	3.17089 (-1)	- 4.48422 (-2)	- 5.76199 (-3)	- 3.15612 (-4)	–	–
8 - 0	52.3372	5.62872 (+0)	2.69400 (-1)	- 7.80898 (-2)	- 1.40938 (-2)	- 1.23486 (-3)	- 3.39746 (-5)	–
7 - 0	52.3372	3.95774 (+0)	4.37216 (-1)	1.35953 (-2)	3.25038 (-3)	6.66057 (-5)	–	–
6 - 0	52.3372	2.63932 (+0)	3.63251 (-1)	- 1.43244 (-2)	8.11499 (-4)	–	–	–
5 - 0	52.3372	2.39984 (+0)	4.44829 (-1)	- 1.42826 (-2)	- 1.53566 (-3)	- 2.53099 (-4)	1.67438 (-5)	1.90303 (-6)
4 - 0	52.3372	1.86306 (+0)	4.90040 (-1)	1.21828 (-2)	4.40861 (-3)	- 5.58066 (-4)	- 8.88669 (-5)	- 2.58811 (-6)
3 - 0	52.3372	1.33300 (+0)	5.61151 (-1)	3.78913 (-3)	8.28793 (-3)	5.50079 (-4)	–	–
2 - 0	52.3372	9.45868 (-1)	6.84962 (-1)	- 1.17630 (-2)	7.39342 (-3)	8.64629 (-4)	1.68263 (-5)	–
1 - 0	52.3372	7.09034 (-1)	7.35786 (-1)	- 7.74556 (-2)	- 6.54135 (-3)	–	–	–
0 - 0	52.3372	6.40222 (-1)	9.24003 (-1)	- 1.71422 (-2)	8.40830 (-4)	2.76026 (-4)	–	–

* $(+1) = 10^1$; $(-1) = 10^{-1}$

TABLE 3. COEFFICIENTS FOR THE REDUCTION FACTORS $R_b^*(O_2)$ IN FORMULA (16)

Band	x_0	a	c_1	c_2	c_3	c_4	c_5	c_6
19 - 0	47.8366	5.11460 (+1)*	5.10382 (-2)	8.73943 (-3)	1.04447 (-3)	5.89092 (-5)	–	–
18 - 0	46.9705	5.00719 (+1)	4.43874 (-2)	5.00297 (-3)	3.79065 (-4)	2.46433 (-5)	–	–
17 - 0	47.1210	5.00818 (+1)	3.80646 (-2)	2.49528 (-3)	- 1.02661 (-5)	–	–	–
16 - 0	47.2689	5.04340 (+1)	4.63249 (-2)	7.09082 (-3)	8.98831 (-4)	5.77473 (-5)	–	–
15 - 0	47.6981	5.03652 (+1)	3.38745 (-2)	3.32142 (-3)	4.32553 (-4)	3.35514 (-5)	–	–
14 - 0	47.8366	5.02938 (+1)	3.51286 (-2)	5.31714 (-3)	8.15685 (-4)	5.34462 (-5)	–	–
13 - 0	48.1071	5.05610 (+1)	4.39864 (-2)	1.26616 (-2)	2.81490 (-3)	2.84044 (-4)	9.79660 (-6)	–
12 - 0	48.3707	5.10442 (+1)	5.99863 (-2)	2.82775 (-2)	9.18649 (-3)	1.52692 (-3)	1.24380 (-4)	4.01234 (-6)
11 - 0	48.7587	5.11875 (+1)	2.84639 (-2)	- 4.66058 (-3)	- 4.55939 (-3)	- 1.20694 (-3)	- 1.34151 (-4)	- 5.33233 (-6)
10 - 0	49.2632	5.16385 (+1)	3.80068 (-2)	8.98509 (-3)	1.73130 (-3)	1.18619 (-4)	- 3.39860 (-6)	- 4.54339 (-7)
9 - 0	49.7590	5.22077 (+1)	4.71498 (-2)	1.56032 (-2)	3.45399 (-3)	3.45446 (-4)	1.23091 (-5)	–
8 - 0	50.1323	5.24801 (+1)	4.04241 (-2)	1.14692 (-2)	2.68444 (-3)	3.24591 (-4)	1.81548 (-5)	3.77777 (-7)
7 - 0	50.9126	5.32532 (+1)	2.92527 (-2)	2.18557 (-3)	- 1.82273 (-4)	- 8.43583 (-5)	- 9.19628 (-6)	- 3.19482 (-7)
6 - 0	51.7482	5.39973 (+1)	2.55970 (-2)	1.37135 (-3)	1.35395 (-5)	–	–	–
5 - 0	52.3372	5.45428 (+1)	2.89681 (-2)	3.89198 (-3)	6.32160 (-4)	6.86338 (-5)	3.25533 (-6)	4.72141 (-8)
4 - 0	52.3372	5.40782 (+1)	1.81043 (-2)	- 9.49775 (-4)	- 3.91127 (-4)	- 2.52678 (-5)	- 4.25174 (-7)	–
3 - 0	52.3372	5.37578 (+1)	1.76096 (-2)	8.60701 (-4)	- 8.73800 (-5)	- 6.32969 (-6)	–	–
2 - 0	52.3372	5.35484 (+1)	1.56696 (-2)	2.24308 (-3)	1.32230 (-4)	2.57769 (-6)	–	–
1 - 0	52.3372	5.32918 (+1)	8.44393 (-3)	1.44896 (-3)	9.75944 (-5)	2.12883 (-6)	–	–
0 - 0	52.3372	5.33607 (+1)	9.95270 (-3)	3.37492 (-3)	5.50237 (-4)	4.24324 (-5)	1.23625 (-6)	–

* $(+1) = 10^1$; $(-1) = 10^{-1}$.

computed every kilometer between the level x_0 and 115 km from the expression

$$\delta = \frac{R_b^* - R_b}{R_b} \times 100\%. \qquad (17)$$

This error can be positive or negative and its average value is practically zero as an obvious consequence of the least-square fitting procedure which leads to the coefficients of Tables 2 and 3. An index of the accuracy of the analytical approximation (16) is then given by the S.D., $s(\%)$ of the errors. The standard deviations s are given in Table 4 for $R_b^*(M)$ and $R_b^*(O_2)$. It can be seen that the approximate expressions R_b^* represent rather well the correct results. The fit for $R_b^*(M)$ is usually better than for $R_b^*(O_2)$. When photodissociation coefficients are computed with $R_b^*(M)$ and $R_b^*(O_2)$ the agreement with the exact computations is such that it is impossible to distinguish both results on graphs like Figs. 7 and 8. This implies that the approximate expressions can be used for modelling purposes, since the resulting error is much smaller than the errors involved in other parameters, such as the solar fluxes and the absorption cross sections of the minor constituents.

TABLE 4. S.D. FOR THE BAND INTERVAL APPROXIMATIONS $R_b^*(M)$ AND $R_b^*(O_2)$

Band	$s[R_b^*(M)]$ (%)	$s[R_b^*(O_2)]$ (%)	Band	$s[R_b^*(M)]$ (%)	$s[R_b^*(O_2)]$ (%)
19 - 0	1.03	2.77	9 - 0	4.99	4.07
18 - 0	2.04	4.55	8 - 0	6.57	3.98
17 - 0	1.27	2.72	7 - 0	2.53	4.82
16 - 0	1.63	1.96	6 - 0	1.14	7.22
15 - 0	0.68	2.74	5 - 0	0.84	4.68
14 - 0	1.67	3.45	4 - 0	0.45	2.92
13 - 0	1.13	2.19	3 - 0	0.86	2.98
12 - 0	0.35	4.47	2 - 0	0.81	1.69
11 - 0	0.88	3.90	1 - 0	0.92	3.60
10 - 0	4.04	2.32	0 - 0	0.40	1.52

It is also possible to justify the validity of our approximation when the solar zenith distance changes and when other atmospheric models are used. Figure 12 shows the temperature distribution in the 45°N U.S. Standard Atmosphere (COESA, 1962) and in the summer and winter models available in the U.S. Standard Atmosphere Supplements (COESA, 1966).

For a specific model, variations of the solar zenith distance imply variations of the O_2 total content. Since the last quantity is temperature dependent, different absorption cross sections should be used in the optical depth given by Equation (5). Figure 12 indicates that, for total contents greater than 10^{18} cm^{-2}, a variation of a factor of 4 in the total content of the 45°N model implies always a temperature variation smaller than 30 K, i.e. a negligible variation in the absorption cross section. Variations of the solar zenith distance between 0 and 75° are, therefore, well represented by total content variations in expression (16). Isolated sunrise and sunset phenomena are better described by detailed computations.

Adoption of other atmospheric models, for example the 45°N July or January models could *a priori* lead to variations in the reduction factors since the temperature distribution is different over the whole height range. The exact reduction factor $R_b(O_2)$ computed for the 6–0 band with Equation (12) is given in Fig. 13 for the three models shown in Fig. 12 and it is clear that the differences are practically negligible. A similar comparison is presented in Fig. 14 for the reduction factor $R_b(M)$ computed for the 9–0 band with Equation (11). It is

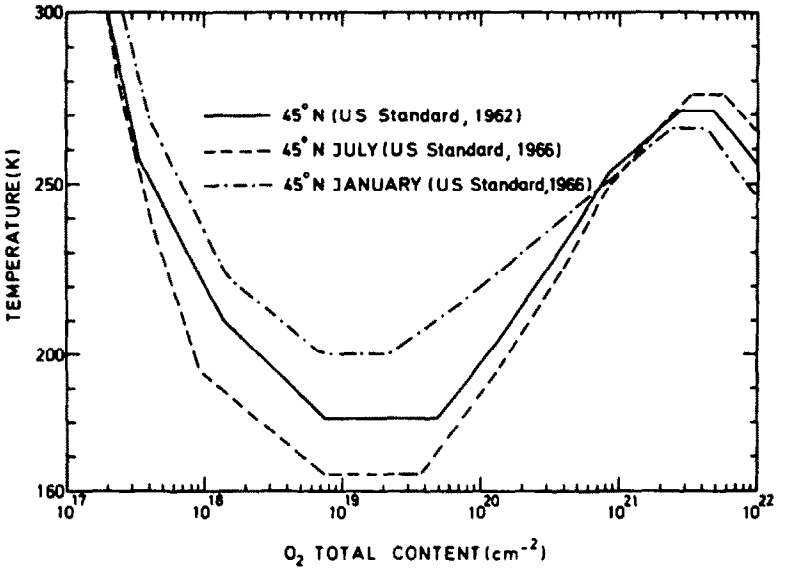

FIG. 12. TEMPERATURE DISTRIBUTION IN THREE 45°N ATMOSPHERIC MODELS AS A FUNCTION OF THE VERTICAL O_2 TOTAL CONTENT.

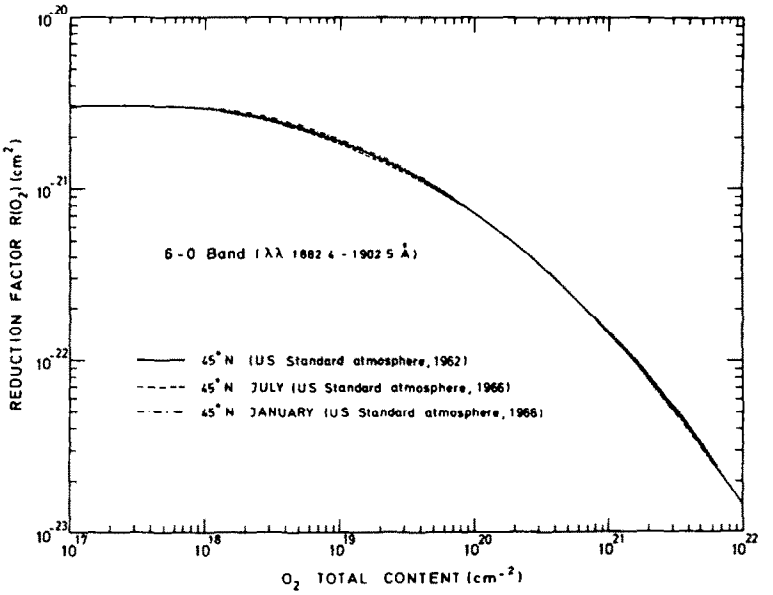

FIG. 13. COMPARISON OF THE REDUCTION FACTOR $R_b(O_2)$ IN THE 6–0 BAND FOR THREE 45°N ATMOSPHERIC MODELS AS A FUNCTION OF THE O_2 TOTAL CONTEST.

only for optical depths greater than 4.6 that sensible differences occur. The bands 6–0 and 9–0 have been chosen for Figs. 13 and 14 since they correspond to relatively large errors (≥5%) in the numerical approximation (see Table 4). It appears, nevertheless, that the numerical coefficients given in Tables 2 and 3, can be used for a wide range of atmospheric models.

5. NUMERICAL APPROXIMATIONS FOR $\Delta\nu = 500\ cm^{-1}$ AND $\Delta\lambda = 10$ Å

The subdivision of the Schumann–Runge spectral range adopted in the preceding sections is based on the physical structure (individual bands) of the absorption cross section of molecular oxygen and the penetration of solar radiation and photodissociation coefficients have been determined using the solar

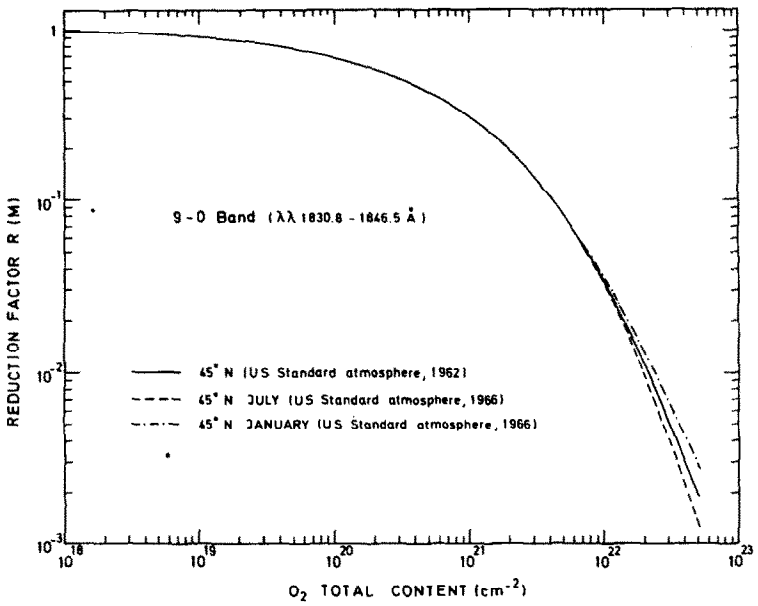

FIG. 14. COMPARISON OF THE REDUCTION FACTOR $R_b(M)$ IN THE 9–0 BAND FOR THREE 45°N ATMOSPHERIC MODELS AS A FUNCTION OF THE O_2 TOTAL CONTENT.

flux available at the top of the atmosphere. Since solar flux measurements are often averaged over specific wavelength or wavenumber intervals, the analysis, which was developed in Section 4, is, therefore, extended for usual applications with 500 cm^{-1} or 10 Å intervals. Expressions (4) to (17) can be used for such an extension when the index b now refers to the wavenumber interval $\Delta\nu = 500\ cm^{-1}$ or to the wavelength interval $\Delta\lambda = 10$ Å and when n_b is the number of subintervals characterized by a width of 0.5 cm^{-1} in the intervals $\Delta\nu$ or $\Delta\lambda$.

The reduction factors $R_{\Delta\nu}(M)$, $R_{\Delta\nu}(O_2)$, $R_{\Delta\lambda}(M)$ and $R_{\Delta\lambda}(O_2)$ are first computed with expressions (11) and (12). Then the coefficients of the analytical approximation (16) are similarly determined as for the band intervals. The approximate reduction factors $R_{\Delta\nu}{}^*(M)$ and $R_{\Delta\nu}{}^*(O_2)$ can now be computed with the coefficients given in Tables 5 and 6, respectively. The computations have been made with the 45°N U.S. Standard Atmosphere (COESA, 1962). The standard deviations for each 500 cm^{-1} interval are given in Table 7. For wavelength intervals of 10 Å, the coefficient of $R_{\Delta\lambda}{}^*(M)$ and $R_{\Delta\lambda}{}^*(O_2)$ are presented in Tables 8 and 9, respectively, with the standard deviations in Table 10. It appears from Tables 4, 7, and 10 that the standard deviation never exceeds 10%. Most values are even smaller than 5%. The accuracy is, however, not identical for any type of subdivision of the

TABLE 5. COEFFICIENTS FOR THE REDUCTION FACTORS $R_{\Delta\nu}{}^*(M)$ ($\Delta\nu = 500\ cm^{-1}$)

Interval (cm^{-1})	x_0	a	c_1	c_2	c_3	c_4	c_5	c_6
56500 - 57000	48.3707	6.84796 (+0)*	5.17316 (-1)	8.59061 (-3)	- 3.72072 (-3)	- 1.50404 (-3)	- 8.50021 (-5)	–
56000 - 56500	49.0127	6.53186 (+0)	6.49898 (-1)	5.81672 (-2)	5.98594 (-3)	–	–	–
55500 - 56000	49.5111	6.84941 (+0)	6.66003 (-1)	- 8.07720 (-3)	- 1.01234 (-2)	- 2.88266 (-4)	1.83032 (-4)	1.20649 (-5)
55000 - 55500	50.1323	6.54328 (+0)	4.94888 (-1)	- 3.45895 (-2)	- 1.12340 (-2)	- 2.22054 (-4)	1.86201 (-4)	1.17659 (-5)
54500 - 55000	50.7790	6.61757 (+0)	4.96086 (-1)	- 4.02125 (-2)	- 1.58932 (-2)	- 2.04106 (-3)	- 7.45240 (-5)	–
54000 - 54500	52.3372	6.46996 (+0)	3.01154 (-1)	- 5.65770 (-2)	- 9.71457 (-3)	- 8.70772 (-4)	- 2.36123 (-5)	–
53500 - 54000	52.3372	5.66059 (+0)	2.88223 (-1)	- 6.36151 (-2)	- 9.79217 (-3)	- 8.87904 (-4)	- 2.61077 (-5)	–
53000 - 53500	52.3372	3.82674 (+0)	4.08489 (-1)	- 6.77337 (-4)	3.02650 (-3)	1.09148 (-4)	–	–
52500 - 53000	52.3372	2.50743 (+0)	3.36617 (-1)	- 4.89806 (-2)	- 3.99197 (-3)	3.19888 (-5)	5.69852 (-5)	3.14619 (-6)
52000 - 52500	52.3372	2.21706 (+0)	4.46436 (-1)	- 2.92693 (-2)	- 1.07835 (-3)	- 4.06946 (-4)	- 4.34128 (-5)	- 1.15593 (-6)
51500 - 52000	52.3372	2.25964 (+0)	4.39618 (-1)	- 5.79418 (-4)	3.61300 (-3)	- 4.70989 (-4)	- 7.80044 (-5)	- 2.38741 (-6)
51000 - 51500	52.3372	1.62727 (+0)	5.25292 (-1)	- 1.36387 (-2)	2.51229 (-3)	- 3.41931 (-4)	- 6.22044 (-5)	- 1.75418 (-6)
50500 - 51000	52.3372	1.15386 (+0)	6.73839 (-1)	- 1.61677 (-2)	4.81976 (-3)	4.44662 (-4)	–	–
50000 - 50500	52.3372	8.37997 (-1)	7.83500 (-1)	- 4.04270 (-2)	2.06058 (-3)	6.63043 (-4)	1.70475 (-5)	–
49500 - 50000	52.3372	7.34395 (-1)	8.69102 (-1)	- 1.21049 (-2)	6.09572 (-3)	9.62943 (-4)	2.57319 (-5)	–
49000 - 49500	52.3372	6.34568 (-1)	9.54356 (-1)	7.95421 (-3)	7.64268 (-3)	9.97614 (-4)	2.47973 (-5)	–

* $(+1) = 10^1$; $(-1) = 10^{-1}$

TABLE 6. COEFFICIENTS FOR THE REDUCTION FACTORS $R_{\Delta\nu}{}^*(O_2)$ ($\Delta\nu = 500\ cm^{-1}$)

Interval (cm^{-1})	x_0	a	c_1	c_2	c_3	c_4	c_5	c_6
56500 - 57000	47.1210	5.02877 (+1)*	4.82356 (-2)	8.27089 (-3)	1.15739 (-3)	7.73906 (-5)	–	–
56000 - 56500	47.8366	5.05677 (+1)	4.16742 (-2)	8.62389 (-3)	1.70708 (-3)	1.66265 (-4)	5.22380 (-6)	–
55500 - 56000	48.3707	5.10464 (+1)	5.91157 (-2)	2.40099 (-2)	6.11691 (-3)	7.01218 (-4)	2.88977 (-5)	–
55000 - 55500	48.6303	5.11271 (+1)	3.29493 (-2)	- 8.68988 (-4)	- 3.42549 (-3)	- 1.09137 (-3)	- 1.34276 (-4)	- 5.72530 (-6)
54500 - 55000	49.2632	5.18149 (+1)	4.03702 (-2)	8.39479 (-3)	1.20197 (-3)	7.45130 (-6)	- 1.34654 (-5)	- 8.01332 (-7)
54000 - 54500	49.8830	5.25076 (+1)	5.05408 (-2)	1.68231 (-2)	3.76192 (-3)	3.86970 (-4)	1.42579 (-5)	–
53500 - 54000	50.3867	5.29051 (+1)	3.70815 (-2)	5.85835 (-3)	7.38473 (-4)	5.21511 (-5)	1.32429 (-6)	–
53000 - 53500	51.3230	5.39594 (+1)	3.69966 (-2)	5.84476 (-3)	7.89350 (-4)	6.37308 (-5)	1.98711 (-6)	–
52500 - 53000	52.1884	5.47078 (+1)	3.47011 (-2)	5.51635 (-3)	8.45727 (-4)	8.53671 (-5)	4.11990 (-6)	6.85472 (-8)
52000 - 52500	52.3372	5.43298 (+1)	2.55053 (-2)	1.66027 (-3)	- 3.21809 (-5)	- 4.82309 (-6)	–	–
51500 - 52000	52.3372	5.43850 (+1)	2.15633 (-2)	- 9.10283 (-4)	- 4.89103 (-4)	- 3.73518 (-5)	- 8.54613 (-7)	–
51000 - 51500	52.3372	5.38929 (+1)	1.91196 (-2)	1.69782 (-4)	- 3.25458 (-4)	- 3.07342 (-5)	- 8.22557 (-7)	–
50500 - 51000	52.3372	5.35620 (+1)	1.69056 (-2)	2.10918 (-3)	8.48166 (-5)	–	–	–
50000 - 50500	52.3372	5.33348 (+1)	1.15487 (-2)	2.14539 (-3)	1.43383 (-4)	2.65172 (-6)	–	–
49500 - 50000	52.3372	5.34000 (+1)	1.13954 (-2)	2.23775 (-3)	2.39814 (-5)	- 3.71615 (-5)	- 3.92715 (-6)	- 1.23474 (-7)
49000 - 49500	52.3372	5.32813 (+1)	5.89039 (-3)	1.16632 (-3)	9.38987 (-5)	2.63348 (-6)	–	–

* $(+1) = 10^1$; $(-1) = 10^{-1}$.

TABLE 7. S.D. FOR THE 500 cm^{-1} APPROXIMATIONS $R_{\Delta\nu}{}^*(M)$ AND $R_{\Delta\nu}{}^*(O_2)$

Interval (cm^{-1})	$\sigma[R^*_{\Delta\nu}(M)]$ (%)	$\sigma[R^*_{\Delta\nu}(O_2)]$ (%)	Interval (cm^{-1})	$\sigma[R^*_{\Delta\nu}(M)]$ (%)	$\sigma[R^*_{\Delta\nu}(O_2)]$ (%)
56500 - 57000	1.37	2.87	52500 - 53000	1.30	6.49
56000 - 56500	0.44	1.53	52000 - 52500	0.94	4.89
55500 - 56000	0.78	4.64	51500 - 52000	0.54	2.60
55000 - 55500	0.99	3.55	51000 - 51500	0.73	2.07
54500 - 55000	1.27	2.36	50500 - 51000	0.39	3.72
54000 - 54500	5.78	4.09	50000 - 50500	0.44	4.67
53500 - 54000	0.76	7.80	49500 - 50000	0.43	0.67
53000 - 53500	2.08	5.18	49000 - 49500	0.40	2.67

Schumann–Runge spectral range. The variability of the standard deviations in the intervals of the same type (band, 500 cm^{-1}, 10 Å) is an indication of the complexity of the structure in the Schumann–Runge bands. In particular when an interval overlaps with two bands, the standard deviation of the approximation is usually higher. For the case of the band intervals, the error increases when one or two band origin of the $v'' = 1$ progression falls in this interval. Finally, it appears that the standard deviation is usually higher for the $R^*(O_2)$ reduction factors as a consequence of the appearance of the O_2 absorption cross section in front of the exponential in equation (12).

The choice of $R_b{}^*$, $R_{\Delta\nu}{}^*$ or $R_{\Delta\lambda}{}^*$ must be guided by the physical problem which is studied and by the precision involved in other parameters such as solar fluxes or absorption cross sections.

CONCLUSION

The penetration of solar radiation in the Schumann–Runge spectral range and the subsequent photodissociation of O_2 and minor constituents require lengthy computations when the

TABLE 8. COEFFICIENTS FOR THE REDUCTION FACTORS $R_{\Delta\lambda}{}^*(M)$ ($\Delta\lambda = 10$ Å)

Interval (Å)	x_0	a	c_1	c_2	c_3	c_4	c_5	c_6
1750 - 1760	48.2394	6.89763 (+0)*	5.29106 (-1)	5.67145 (-2)	1.60166 (-2)	4.44083 (-3)	8.40779 (-4)	5.01998 (-5)
1760 - 1770	48.3707	6.67932 (+0)	5.63736 (-1)	6.28478 (-2)	1.89533 (-2)	3.28456 (-3)	4.01096 (-4)	1.88421 (-5)
1770 - 1780	48.7587	6.49036 (+0)	6.72570 (-1)	5.97308 (-2)	6.21615 (-3)	–	–	–
1780 - 1790	49.1384	6.46131 (+0)	6.58662 (-1)	3.47022 (-3)	- 1.09451 (-2)	- 1.38507 (-3)	3.16800 (-5)	5.81154 (-6)
1790 - 1800	49.5111	6.74455 (+0)	6.60024 (-1)	1.87822 (-2)	- 3.03357 (-3)	4.64532 (-4)	2.25992 (-4)	1.32604 (-5)
1800 - 1810	49.3872	6.67780 (+0)	6.72745 (-1)	3.81980 (-3)	- 1.77364 (-2)	- 3.49056 (-3)	- 1.67210 (-4)	–
1810 - 1820	50.2588	6.56436 (+0)	5.69372 (-1)	- 2.28925 (-2)	- 1.11467 (-2)	- 4.74513 (-4)	1.48286 (-4)	1.00247 (-5)
1820 - 1830	50.9126	6.66317 (+0)	5.84378 (-1)	- 1.51955 (-2)	- 2.28127 (-3)	2.02568 (-4)	6.49102 (-5)	2.96791 (-6)
1830 - 1840	50.6468	7.09088 (+0)	6.60362 (-1)	5.00243 (-2)	4.95675 (-3)	3.27498 (-5)	–	–
1840 - 1850	52.3372	6.13304 (+0)	4.07111 (-1)	- 3.88234 (-2)	- 1.21181 (-2)	- 1.36375 (-3)	- 4.28120 (-5)	–
1850 - 1860	52.0404	6.73366 (+0)	3.01091 (-1)	- 9.64724 (-2)	- 8.64758 (-3)	5.31552 (-4)	1.30406 (-4)	5.30821 (-6)
1860 - 1870	52.3372	5.02651 (+0)	2.68855 (-1)	- 4.51007 (-2)	- 8.30801 (-3)	- 9.71517 (-4)	- 3.28893 (-5)	–
1870 - 1880	52.3372	3.35811 (+0)	3.58322 (-1)	- 2.87486 (-2)	6.41145 (-3)	5.28891 (-4)	- 3.36908 (-5)	- 2.75414 (-6)
1880 - 1890	52.3372	4.95636 (+0)	3.80234 (-1)	- 1.66185 (-2)	- 3.41767 (-3)	- 6.57498 (-4)	- 2.72453 (-5)	–
1890 - 1900	52.3372	1.97465 (+0)	4.75264 (-1)	- 1.09092 (-2)	8.90634 (-3)	1.46761 (-4)	- 1.20909 (-4)	- 6.49139 (-6)
1900 - 1910	52.3372	5.39459 (+0)	4.64390 (-1)	- 1.53222 (-2)	- 2.31276 (-3)	- 2.73232 (-4)	2.25483 (-5)	2.11368 (-6)
1910 - 1920	52.3372	1.81992 (+0)	5.08220 (-1)	- 1.13600 (-2)	1.14126 (-2)	3.40578 (-4)	- 1.34649 (-4)	- 7.55946 (-6)
1920 - 1930	52.3372	3.06585 (+0)	4.02512 (-1)	7.83849 (-3)	6.28983 (-3)	- 1.73235 (-4)	- 6.29372 (-5)	- 2.21684 (-6)
1930 - 1940	52.3372	1.85962 (+0)	3.64911 (-1)	- 1.14010 (-1)	- 6.34984(-3)	–	–	–
1940 - 1950	52.3372	1.51564 (+0)	5.28202 (-1)	9.55208 (-3)	7.91041 (-3)	4.34474 (-4)	–	–
1950 - 1960	52.3372	1.60222 (+0)	5.11932 (-1)	- 2.61144 (-2)	4.95775 (-3)	1.65694 (-4)	- 5.11283 (-5)	- 2.51486 (-6)
1960 - 1970	52.3372	9.71685 (-1)	5.12511 (-1)	- 1.62117 (-1)	- 1.46720 (-2)	- 2.77276 (-4)	–	–
1970 - 1980	52.3372	1.37699 (+0)	6.26462 (-1)	- 7.08644 (-3)	5.68126 (-3)	3.99301 (-4)	–	–
1980 - 1990	52.3372	8.84565 (-1)	7.26460 (-1)	- 7.76640 (-2)	- 4.84921 (-3)	7.28988 (-5)	–	–
1990 - 2000	52.3372	8.66214 (-1)	1.00177 (+0)	4.51336 (-2)	1.03045 (-2)	6.41182 (-4)	–	–
2000 - 2010	52.3372	8.84123 (-1)	9.31330 (-1)	1.04577 (-2)	5.95152 (-3)	4.78163 (-4)	–	–
2010 - 2020	52.3372	5.77989 (-1)	1.00667 (+0)	1.97533 (-2)	6.32736 (-3)	5.00822 (-4)	–	–
2020 - 2030	52.3372	6.94593 (-1)	1.08332 (+0)	5.28970 (-2)	1.05677 (-2)	6.66814 (-4)	–	–
2030 - 2040	52.3372	6.51117 (-1)	1.03060 (+0)	3.03642 (-2)	7.70258 (-3)	5.57472 (-4)	–	–
2040 - 2050	52.3372	6.16626 (-1)	1.05655 (+0)	4.11376 (-2)	9.08845 (-3)	6.15747 (-4)	–	–

* $(+1) = 10^1$; $(-1) = 10^{-1}$.

TABLE 9. COEFFICIENTS FOR THE REDUCTION FACTORS $R_{\Delta\lambda}{}^*(O_2)$ ($\Delta\lambda = 10$ Å)

Interval (Å)	x_o	a	c_1	c_2	c_3	c_4	c_5	c_6
1750 - 1760	46.8173	4.98284 (+1)*	3.87574 (-2)	9.17924 (-3)	4.07267 (-3)	7.80514 (-4)	4.73601 (-5)	–
1760 - 1770	47.1210	5.02232 (+1)	5.00733 (-2)	1.53258 (-2)	5.59964 (-3)	1.18880 (-3)	1.22784 (-4)	4.97235 (-6)
1770 - 1780	47.6981	5.03908 (+1)	3.98650 (-2)	6.50488 (-3)	9.45939 (-4)	5.98214 (-5)	–	–
1780 - 1790	48.1071	5.06646 (+1)	4.08847 (-2)	8.19503 (-3)	1.26973 (-3)	7.54648 (-5)	–	–
1790 - 1800	48.3707	5.09270 (+1)	3.94964 (-2)	7.51466 (-3)	1.15582 (-3)	6.89678 (-5)	–	–
1800 - 1810	48.3707	5.09869 (+1)	3.91533 (-2)	6.60149 (-3)	9.50775 (-4)	5.79830 (-5)	–	–
1810 - 1820	49.0127	5.15103 (+1)	3.79382 (-2)	7.42674 (-3)	1.33775 (-3)	1.17154 (-4)	3.26677 (-6)	–
1820 - 1830	49.6350	5.20520 (+1)	4.30321 (-2)	1.06279 (-2)	2.12653 (-3)	2.59263 (-4)	1.68657 (-5)	4.53469 (-7)
1830 - 1840	49.1384	5.16936 (+1)	4.45972 (-2)	1.22676 (-2)	2.54289 (-3)	2.28142 (-4)	3.82202 (-6)	- 2.80316 (-7)
1840 - 1850	50.1323	5.24937 (+1)	3.90603 (-2)	1.11385 (-2)	2.54012 (-3)	2.60706 (-4)	9.28528 (-6)	–
1850 - 1860	50.2588	5.29072 (+1)	5.14423 (-2)	1.44397 (-2)	2.67736 (-3)	2.67504 (-4)	1.25948 (-5)	2.01172 (-7)
1860 - 1870	50.1323	5.28284 (+1)	4.49545 (-2)	1.27869 (-2)	3.02669 (-3)	3.72476 (-4)	2.06245 (-5)	3.98251 (-7)
1870 - 1880	51.7482	5.43478 (+1)	3.66791 (-2)	4.17660 (-3)	1.47417 (-4)	- 2.12345 (-6)	–	–
1880 - 1890	50.7790	5.36676 (+1)	4.53543 (-2)	1.03020 (-2)	1.83785 (-3)	1.68931 (-4)	5.68145 (-6)	–
1890 - 1900	52.3372	5.42884 (+1)	2.74950 (-2)	2.04873 (-3)	- 2.03154 (-4)	- 3.09675 (-5)	- 8.92868 (-7)	–
1900 - 1910	51.3230	5.42585 (+1)	4.48073 (-2)	9.45018 (-3)	1.70178 (-3)	1.84340 (-4)	9.38967 (-6)	1.65569 (-7)
1910 - 1920	52.3372	5.40122 (+1)	2.15554 (-2)	- 5.37363 (-4)	- 7.31229 (-4)	- 6.23199 (-5)	3.23266 (-8)	9.66567 (-8)
1920 - 1930	52.3372	5.50572 (+1)	2.85247 (-2)	4.17517 (-4)	- 2.50128 (-4)	- 1.40539 (-5)	- 5.24836 (-8)	–
1930 - 1940	52.3372	5.40083 (+1)	2.20002 (-2)	2.62723 (-5)	- 4.44432 (-4)	1.43133 (-6)	5.92530 (-6)	2.88189 (-7)
1940 - 1950	52.3372	5.39047 (+1)	1.87485 (-2)	6.27526 (-4)	- 9.40523 (-5)	- 3.01527 (-6)	1.73142 (-7)	–
1950 - 1960	52.3372	5.38956 (+1)	2.19236 (-2)	1.49760 (-3)	- 1.71685 (-4)	- 2.35142 (-5)	- 6.73216 (-7)	–
1960 - 1970	52.3372	5.35390 (+1)	1.86689 (-2)	3.28509 (-3)	4.49567 (-5)	- 2.01682 (-5)	- 8.56470 (-7)	–
1970 - 1980	52.3372	5.37112 (+1)	1.87544 (-2)	1.38674 (-3)	- 1.29624 (-4)	- 2.08988 (-5)	- 7.17849 (-7)	–
1980 - 1990	52.3372	5.33989 (+1)	1.43302 (-2)	2.93594 (-3)	2.02428 (-4)	3.54629 (-6)	–	–
1990 - 2000	52.3372	5.34105 (+1)	1.39964 (-2)	3.91794 (-3)	5.59879 (-4)	3.79849 (-5)	8.20535 (-7)	- 1.12618 (-8)
2000 - 2010	52.3372	5.33760 (+1)	1.26958 (-2)	2.61779 (-3)	1.71905 (-4)	- 6.65420 (-6)	- 1.24190 (-6)	- 4.01984 (-8)
2010 - 2020	52.3372	5.32539 (+1)	5.63802 (-3)	1.00563 (-3)	6.26682 (-5)	9.68210 (-7)	–	–
2020 - 2030	52.3372	5.33438 (+1)	9.34520 (-3)	3.02825 (-3)	4.79717 (-4)	3.61907 (-5)	1.03344 (-6)	–
2030 - 2040	52.3372	5.32898 (+1)	6.24672 (-3)	1.50722 (-3)	1.78772 (-4)	1.09906 (-5)	2.86579 (-7)	–
2040 - 2050	52.3372	5.32468 (+1)	3.39325 (-3)	4.03809 (-4)	8.51021 (-6)	- 5.21570 (-7)	–	–

* $(+1) = 10^1$; $(-1) = 10^{-1}$.

TABLE 10. S.D. FOR THE 10 Å APPROXIMATIONS $R_{\Delta\lambda}{}^*(M)$ AND $R_{\Delta\lambda}{}^*(O_2)$

Interval (Å)	$s[R^*_{\Delta\lambda}(M)]$ (%)	$s[R^*_{\Delta\lambda}(O_2)]$ (%)	Interval (Å)	$s[R^*_{\Delta\lambda}(M)]$ (%)	$s[R^*_{\Delta\lambda}(O_2)]$ (%)
1750 - 1760	2.31	5.36	1900 - 1910	3.23	4.18
1760 - 1770	0.80	1.83	1910 - 1920	1.33	5.38
1770 - 1780	0.68	2.09	1920 - 1930	0.76	3.78
1780 - 1790	1.12	3.85	1930 - 1940	2.47	6.88
1790 - 1800	1.13	4.31	1940 - 1950	0.44	3.08
1800 - 1810	0.97	5.73	1950 - 1960	1.55	5.28
1810 - 1820	1.19	5.44	1960 - 1970	1.13	9.37
1820 - 1830	2.38	3.74	1970 - 1980	0.57	1.91
1830 - 1840	4.74	2.58	1980 - 1990	0.48	5.38
1840 - 1850	5.11	3.31	1990 - 2000	0.56	1.39
1850 - 1860	3.89	2.96	2000 - 2010	0.26	1.48
1860 - 1870	5.28	2.92	2010 - 2020	0.09	3.95
1870 - 1880	2.18	6.43	2020 - 2030	0.26	1.38
1880 - 1890	3.36	3.99	2030 - 2040	0.09	2.63
1890 - 1900	0.76	5.97	2040 - 2050	0.12	4.13

detailed structure of the O_2 absorption cross section is taken into account. Since the resulting physical effect is important over a great height range from the lower thermosphere down to the stratosphere (see Fig. 9), numerical approximations have been developed for a wide range of practical applications.

The introduction of reduction factors provides a simple technique for the calculation of the attenuation of solar radiation. Photodissociation of minor constituents is then easily computed when their absorption cross sections can be approximated by constant values over each interval (band, 500 cm^{-1}, 10 Å) in the Schumann–Runge spectral range. It is, however, necessary to average the solar flux available at the top of the atmosphere over each spectral interval covered by the reduction factors. This excludes, therefore, calculations of photodissociation of minor constituents with a rotational structure in their absorption cross sections as NO, for example (Cieslik and Nicolet, 1973).

Adoption of the analytical approximation given by expression (16) allows a direct computation of the reduction factors as a function of the O_2 total content. Since solar fluxes can be averaged over different intervals (band, 500 cm^{-1} or 10 Å) the numerical coefficients required for the reduction factors have been computed for each type of interval over the Schumann–Runge spectral range (see Tables 2, 3, 5, 6, 8 and 9). When a specific spectral interval is adopted, it is easy to develop a computer subroutine for the reduction factors. Such a subroutine requires the storage of 256, 320, or 480 coefficients when the adopted spectral interval is respectively 500 cm^{-1}, "band" or 10 Å. The total photodissociation coefficients are obtained by a simple summation over the spectral intervals of the Schumann–Runge system.

The same set of coefficients can be used for different solar zenith distances and for a wide range of atmospheric models. Furthermore, the numerical coefficients do not depend on the values adopted for the solar fluxes and for the average absorption coefficients of the minor constituents. Absorption by atmospheric ozone is easily taken into account

through the factor $\exp[-\tau(O_3)]$ in expressions (13)–(15).

In summary, it appears that a simple procedure is now available for the analysis of absorption and photodissociation in the spectral range of the Schumann–Runge bands of molecular oxygen.

Acknowledgement—I wish to thank Prof. M. Nicolet for the constructive discussions during the preparation of this paper.

REFERENCES

Ackerman, M. (1971). Ultraviolet solar radiation related to mesospheric processes, in *Mesospheric Models and Related Experiments* (Ed. G. Fiocco), p. 149. Reidel, Dordrecht, Holland.

Ackerman, M., Biaumé, F. and Kockarts, G. (1970). Absorption cross sections of the Schumann–Runge bands of molecular oxygen. *Planet. Space Sci.* **18,** 1639.

Allison, A. C., Dalgarno, A. and Pasachoff, N. W. (1971). Absorption by vibrationally excited molecular oxygen in the Schumann–Runge continuum. *Planet. Space Sci.* **19,** 1463.

Anderson, J. G. (1971). Rocket-borne ultraviolet spectrometer measurement of OH resonance fluorescence with a diffusive transport model for mesospheric photochemistry, *J. geophys. Res.* **71,** 4634.

Banks, P. M. and Kockarts, G. (1973). *Aeronomy, Part A*, p. 182. Academic Press, N.Y.

Biaumé, F. (1972a). Structure de rotation des bandes 0–0 à 13–0 du système de Schumann–Runge de l'oxygène moléculaire, pp. 66. *Acad. R. Belg. Mém. Cl. Sci.* **40.**

Biaumé, F. (1972b). Détermination de la valeur absolue de l'absorption dans les bandes du système de Schumann–Runge de l'oxygène moléculaire, pp. 270. *Aeron. Acta A* **100,** Inst. Aéronomie Spatiale, Bruxelles.

Biaumé, F. (1973). Nitric acid vapour absorption cross-section spectrum and its photodissociation in the stratosphere. *J. Photochem.* **2,** 139.

Brinkmann, R. T. (1969). Dissociation of water vapor and evolution of oxygen in the terrestrial atmosphere. *J. geophys. Res.* **74,** 5355.

Brinkmann, R. T. (1971). Photochemistry and the escape efficiency of terrestrial hydrogen, in *Mesospheric Models and Related Experiments* (Ed. G. Fiocco), p. 89. Reidel, Dordrecht, Holland.

Cieslik, S. and Nicolet, M. (1973). The aeronomic dissociation of nitric oxide. *Planet. Space Sci.* **21,** 925.

COESA (Committee for the Extension to the Standard Atmosphere) (1962). *The U.S. Standard Atmosphere, 1962*, U.S. Government Printing Office, Washington, DC.

COESA (1966). *The U.S. Standard Atmosphere Supplements, 1966*, U.S. Government Printing Office, Washington, DC.

Creek, D. M. and Nicholls, R. W. (1975). A comprehensive re-analysis of the $O_2(B\,^3\Sigma_u^- - X\,^3\Sigma_g^-)$ Schumann–Runge band system. *Proc. R. Soc. London* (A) **341,** 517.

Fang, T.-M., Wofsy, S. C. and Dalgarno, A. (1974). Opacity distribution functions and absorption in Schumann–Runge bands of molecular oxygen. *Planet. Space Sci.* **22,** 413.

Herzberg, G. (1950). Molecular Spectra and Molecular Structure. I Spectra of diatomic molecules 2nd Edn., p. 122. Reinhold, NY.

Hudson, R. D. and Mahle, S. H. (1972). Photodissociation rates of molecular oxygen in the mesosphere and lower thermosphere. *J. geophys. Res.* **77,** 2902.

Huebner, R. H., Celotta, R. J., Mielczarek, S. R. and Kuyatt, C. E. (1975). Apparent oscillator strengths for molecular oxygen derived from electron-loss measurements. *J. Chem. Phys.* **63,** 241.

Jarmain, W. R. and Nicholls, R. W. (1967). A theoretical study of the $v'' = 0$, 1, 2 progressions of bands and adjoining photodissociation continua of the O_2 Herzberg I system. *Proc. Phys. Soc.* **90,** 545.

Julienne, P. S. and Krauss, M. (1975). Predissociation of the Schumman–Runge bands of O_2. *J. Molec. Spectrosc.* **56,** 270.

Kockarts, G. (1971). Penetration of solar radiation in the Schumann–Runge bands of molecular oxygen, in *Mesospheric Models and Related Experiments* (Ed. G. Fiocco), p. 160. Reidel, Dordrecht, Holland.

Kockarts, G. (1972). Absorption par l'oxygène moléculaire dans les bandes de Schumann–Runge, pp. 195. *Aeron. Acta* A **107,** Fasc. I, Inst. Aéronomie Spatiale, Bruxelles.

Nicolet, M. (1971). Aeronomical reactions of hydrogen and ozone, in *Mesospheric Models and Related Experiments* (Ed. G. Fiocco), p. 1. Reidel, Dordrecht, Holland.

Nicolet, M. (1975). Atmospheric ozone: an introduction to its study. *Rev. Geophys. Space Phys.* **13,** 593.

Nicolet, M. and Peetermans, W. (1972). The production of nitric oxide in the stratosphere by oxidation of nitrous oxide. *Annls. Géophys.* **28,** 751.

Park, J. H. (1974). The equivalent mean absorption cross sections for the O_2 Schumann–Runge bands: application to the H_2O and NO photodissociation rates. *J. atmos. Sci.* **31,** 1893.

Samain, D., Bonnet, R. M., Gayet, R. and Lizambert, C. (1975). Stigmatic spectra of the sun between 1200 Å and 2100 Å. *Astron. Astrophys.* **39,** 71.

Samain, D. and Simon, P. C. (1976). Solar flux determination in the spectral range 150–210 mm. *Solar Phys.*

Shemansky, D. E. (1972). CO_2 extinction coefficient 1700–3000 Å. *J. Chem. Phys.* **56,** 1582.

Simon, P. C. (1976). Extraterrestrial solar fluxes related to aeronomic processes. *Planet. Space Sci.*

Whitten, R. C. and Turco, R. P. (1974). Perturbations of the stratosphere and mesosphere by aerospace vehicles. *AIAA J.* **12,** 1110.